

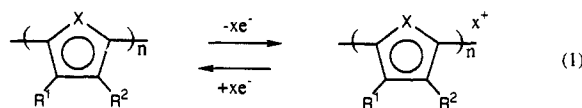
Potential Dependence of the Conductivity of Highly Oxidized Polythiophenes, Polypyrroles, and Polyaniline: Finite Windows of High Conductivity

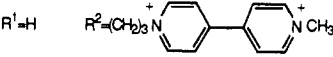
David Ofer, Richard M. Crooks, and Mark S. Wrighton*

Contribution from the Department of Chemistry, Massachusetts Institute of Technology, Cambridge, Massachusetts 02139. Received April 6, 1990

Abstract: In situ measurements of the relative conductivity of polythiophenes, polyaniline, and polypyrroles as a function of electrochemical potential reveal that they have finite potential dependent windows of high conductivity. Further, the high conductivity is found where charge is injected or withdrawn from the polymer. The polymers studied, polyaniline and I-VI, are prepared by anodic polymerization onto microelectrode arrays of the appropriate monomer: thiophene (I), 3-methylthiophene (II), 3-phenylthiophene (III), 1-methyl-1'-(3-(thiophene-3-yl)propyl)-4,4'-bipyridinium (IV), 3,4-dimethylpyrrole (V), and *N*-methylpyrrole (VI). The use of a liquid SO₂/electrolyte medium as the electrochemical solvent makes it possible to define the window of high conductivity, because it allows the polymers to be reversibly oxidized to a greater extent than has previously been achieved. The conductivities of I-IV increase by at least 10⁶-10⁹ when they are oxidized from neutral to the potential of maximum conductivity and then decrease by 10¹-10⁴ when they are further oxidized to the greatest extent possible without irreversible degradation in liquid SO₂/electrolyte. Cyclic voltammetry indicates that IV is oxidized by ~0.3 electron per thiophene repeat unit at the potential of maximum conductivity and by ~0.5 electron per repeat unit at the most positive potential accessible without irreversible degradation. Visible-near-infrared absorption spectroscopy of II at the most positive potential accessible is similar to that at the potential of maximum conductivity, the spectrum having a broad peak extending into the infrared. For thiophene-based polymers I, II, III, and IV, the maximum conductivities are approximately 10⁻¹, 10, 5 × 10⁻², and 5 × 10⁻³ Ω⁻¹ cm⁻¹, respectively, and the widths of the windows of high conductivity are 0.77, 0.98, 0.65, and 0.47 V, respectively. The trend for both properties is II > I > III > IV, consistent with theoretical considerations relating conductivity, band width, and carrier delocalization. Polyaniline undergoes large, reversible, potential dependent changes in conductivity in liquid SO₂/electrolyte in the apparent absence of a protonation/deprotonation mechanism. Conductivity increases by at least 10⁸ upon oxidizing polyaniline from neutral to maximally conducting and decreases by at least 10⁸ when polyaniline is further oxidized in the cyclic voltammogram. Polyaniline can be taken to ~+3.8 V vs SCE in liquid SO₂/electrolyte without irreversible degradation. Visible-near-infrared spectroscopy shows that fully oxidized polyaniline absorbs only at high energy with no absorption at the low energy end of the near infrared. Potential dependent windows of high conductivity and cyclic voltammetry for pyrrole-based polymers V and VI are similar to those for thiophene-based polymers I-IV.

In this paper we report the potential dependence of the conductivity of thiophene-based polymers I-IV and pyrrole-based polymers V and VI. Our results show that all of the polymers have a finite potential window of high conductivity when they are electrochemically oxidized in low-temperature SO₂/electrolyte media (eq 1). In all cases the polymers show sufficiently reversible

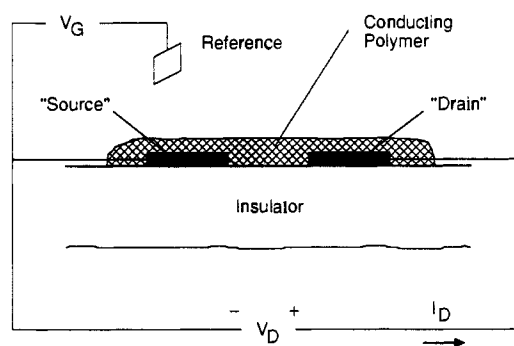


I	X=S	R ¹ =H	R ² =H
II	X=S	R ¹ =H	R ² =CH ₃
III	X=S	R ¹ =H	R ² =C ₆ H ₅
IV	X=S	R ¹ =H	R ² = 
V	X=NH	R ¹ =CH ₃	R ² =CH ₃
VI	X=NCH ₃	R ¹ =H	R ² =H

oxidation that firm conclusions can be drawn concerning the potential dependence of the conductivity. We compare the behavior of I-VI to that of polyaniline, which has previously been shown to have a finite potential window of high conductivity.¹

Microelectrode arrays have been particularly useful as analytical tools for making in situ measurements of potential dependent changes in the conductivity of materials.² Arrays of closely spaced (~1 μm), individually addressable, band (~2 μm × 50 μm × 0.1 μm thick) microelectrodes derivatized with conducting poly-

Scheme 1. Configuration of a Conducting Polymer-Based Transistor*



* Two microelectrodes, called source and drain, are connected with a conducting polymer and a small fixed potential, V_D , is maintained between them. At the same time, their potential vs a reference electrode, V_G , is varied, thus changing the state of charge of the polymer and therefore its conductivity. When the polymer is conducting, significant drain current, I_D , flows between the source and the drain, but when the polymer is insulating negligible drain current flows. I_D is directly proportional to the conductivity of the polymer. Thus, a plot of I_D vs V_G gives relative conductivity vs potential.

mers and operated in a transistor-like configuration can be used to measure the potential dependence of the conductivity of the polymer (Scheme 1).^{1,3,4} The small size of the microelectrodes and the spacing between them is advantageous for two reasons.

(1) Paul, E. W.; Ricco, A. J.; Wrighton, M. S. *J. Phys. Chem.* **1985**, *89*, 1441.

(2) Natan, M. J.; Wrighton, M. S. In *Progress in Inorganic Chemistry*; Lippard, S. J., Ed.; John Wiley and Sons: New York, 1989; Vol. 37.

(3) Kittlesen, G. P.; White, H. S.; Wrighton, M. S. *J. Am. Chem. Soc.* **1984**, *106*, 7389.

(4) Thackeray, J. W.; White, H. S.; Wrighton, M. S. *J. Phys. Chem.* **1985**, *89*, 5133.

* Author to whom correspondence should be addressed.

First, as electrode area (and polymer film area and thickness) is decreased, accurate potential control can be maintained at more rapid scan rates and in more resistive media:⁵ measurements can be made quickly in potential regions where the polymer degrades, and/or the solvent medium can be cooled to slow degradation. Second, closely spaced microelectrodes connected with minimal quantities of conducting polymer show amplification⁶ at the frequencies or scan rates used here: I_D is from one to four orders of magnitude larger than faradaic or gate currents, and it can therefore be easily measured even at fast scan rates.

In $\text{CH}_3\text{CN}/0.1 \text{ M } [(n\text{-Bu})_4\text{N}]\text{ClO}_4$, II has very high conductivity at the most positive potential to which the polymer can be taken without irreversible chemical degradation.⁴ Similar results have been obtained for polypyrrole.^{3,7} In contrast, polyaniline was found to have a finite window of high conductivity bounded by the potential region over which it is durable in acidic aqueous and solid electrolyte media,^{1,8} undergoing a transition from insulating to conducting as it is oxidized and then becoming insulating again at the positive potential limit.

More recently we have exploited the properties of less commonly used solvent/electrolyte systems to extend the potential range of chemical durability for highly oxidized and highly reduced conducting polymers. Liquid SO_2 as an electrochemical solvent has been shown to have a useful potential window with an extremely positive limit ($\sim +4.5 \text{ V}$ vs SCE with $[(n\text{-Bu})_4\text{N}]\text{AsF}_6$ electrolyte),⁹ and to be a particularly good solvent for generating highly oxidized species without chemical degradation.¹⁰ It has been reported that polyacetylene is durable to a higher extent of oxidation in liquid SO_2 than in propylene carbonate.¹¹ Polyaniline can be reversibly oxidized in liquid SO_2 ,¹² but the extent of oxidation has not been measured. In a preliminary communication¹³ we reported that I and II have finite potential windows of high conductivity in liquid $\text{SO}_2/0.1 \text{ M } [(n\text{-Bu})_4\text{N}]\text{PF}_6$, and in this respect their behavior is closer to that of polyaniline than was previously demonstrated. Experiments in liquid NH_3 ¹⁴ have revealed that II also has a finite potential window of high conductivity when it is electrochemically reduced. In this paper we give a full account of the previously reported oxidation of I and II and extend our work to other thiophene and pyrrole-based polymers and to polyaniline. In addition to liquid SO_2 , CH_2Cl_2 has been used as an electrochemical solvent in some cases. Our findings show that a finite potential window of high conductivity is a general feature of organic conducting polymers. Moreover, the potential region of high conductivity is always associated with a region where movement of the potential is accompanied by charge or discharge of the polymer, i.e. high conductivity is found at potentials where the polymer is redox active.

High conductivity in oxidized or reduced conjugated polymers is ascribed to the movement of delocalized charges and associated structural deformations along and between polymer chains.¹⁵ In this case high conductivity should only occur when the polymer contains both charged sites and uncharged sites to which the charges can move. Indeed it has been shown that polyaniline is oxidized to an extent of approximately 0.5 electron per aniline repeat unit at the potential of its maximum conductivity, and to an extent of about 1.0 electron per repeat unit when it is most

oxidized and insulating.¹⁶ In this respect polyaniline is much like the segregated stack organic charge transfer salts such as those of tetracyanoquinodimethane and various electron donors, which are highly conducting only when in a "mixed valence" state of fractional charge per molecule.¹⁷ Theoretical calculations suggest that, in a number of conjugated polymers, the highest occupied electronic band has a finite width with at least a large fraction of the electrons being electrochemically accessible.^{18,19} Therefore the observation of finite potential windows of high conductivity in conjugated organic polymers is consistent with the theoretical expectation that it should be possible to oxidize them to an extent sufficient to render them nonconducting, and it suggests that they bear a general similarity to organic charge transfer salts in that they are highly conducting only in "mixed valence" states of fractional charge per repeat unit. This also makes them similar to conventional redox polymers, which are defined as ones where the charges are highly localized on individual redox centers as in polyvinylferrocene²⁰ or polyviologen.²¹ However, such systems²⁰⁻²² represent an extreme among the electronically conducting polymers. Conductivity occurs via self-exchange processes between electronically non-interacting sites. Nonetheless, like polyaniline and the organic charge transfer salts, the "conductivity" of the conventional redox polymers is maximum when there are oxidized and reduced sites.²³

Experimental Section

Chemicals. 3-Methylthiophene (Aldrich) was used as received. 2,2'-Bithiophene (Aldrich) and 3-phenylthiophene²⁴ were sublimed prior to use. 1-Methyl-1'-(3-(thiophene-3-yl)propyl)-4,4'-bipyridinium·2PF₆⁻ was recrystallized from H_2O .²⁵ 3,4-Dimethylpyrrole was used as received from Professor S. L. Buchwald²⁶ and was stored under Ar in a freezer. *N*-Methylpyrrole (Aldrich) was distilled and stored under Ar in a refrigerator. Aniline (Aldrich) was used as received. $[(n\text{-Bu})_4\text{N}]\text{PF}_6$ was recrystallized from MeOH, dried at 120 °C and 10^{-2} Torr for 1 day, and stored under Ar. $[(n\text{-Bu})_4\text{N}]\text{AsF}_6$ was precipitated by mixing aqueous solutions of $[(n\text{-Bu})_4\text{N}]\text{Br}$ and LiAsF_6 , recrystallized from acetone/water, dried at 100 °C and 10^{-1} Torr, and stored in an inert atmosphere drybox. Commercial HPLC grade CH_3CN was used as received. CH_2Cl_2 (Mallinkrodt analytical grade) was used from freshly opened bottles with experiments being run under an Ar atmosphere with Woelm activity I neutral alumina added to the CH_2Cl_2 /electrolyte. Alternatively, the CH_2Cl_2 was distilled from P_2O_5 and stored under Ar with experiments being run in an inert atmosphere drybox. SO_2 (Matheson anhydrous 99.98%) was bubbled through concentrated H_2SO_4 and either (experiments with $[(n\text{-Bu})_4\text{N}]\text{PF}_6$ electrolyte) passed through Woelm activity I neutral alumina and condensed into an electrochemical

(16) Orata, D.; Buttry, D. A. *J. Am. Chem. Soc.* **1987**, *109*, 3574.

(17) (a) Torrance, J. B. *Acc. Chem. Res.* **1979**, *12*, 79. (b) Torrance, J. B. *Mol. Cryst. Liq. Cryst.* **1985**, *126*, 55. (c) Ward, M. D. In *Electroanalytical Chemistry: A Series of Advances*; Bard, A. J., Ed.; Marcel Dekker: New York, 1989; Vol. 16.

(18) Brédas, J. L.; Elsenbaumer, R. L.; Chance, R. R.; Silbey, R. *J. Chem. Phys.* **1983**, *78*, 5656.

(19) (a) Boudreaux, D. S.; Chance, R. R.; Wolf, J. F.; Shacklette, L. W.; Brédas, J. L.; Thémans, B.; André, J. M.; Silbey, R. *J. Chem. Phys.* **1986**, *85*, 4584. (b) Bakhshi, A. K.; Ladik, J.; Seel, M. *Phys. Rev. B* **1987**, *35*, 704. (c) Stafström, S.; Brédas, J. L. *Mol. Cryst. Liq. Cryst.* **1988**, *160*, 405.

(20) (a) Smith, T. W.; Kuder, J. E.; Wychik, D. *J. Polym. Sci.* **1976**, *14*, 2433. (b) Merz, A.; Bard, A. J. *J. Am. Chem. Soc.* **1978**, *100*, 3222. (c) Nowak, R.; Schultz, F. A.; Umaña, M.; Abruña, H.; Murray, R. W. *J. Electroanal. Chem.* **1978**, *94*, 219.

(21) (a) Bookbinder, D. C.; Wrighton, M. S. *J. Am. Chem. Soc.* **1980**, *102*, 5123. (b) Abruña, H. D.; Bard, A. J. *J. Am. Chem. Soc.* **1981**, *103*, 6898. (c) Killman, K. W.; Murray, R. W. *J. Electroanal. Chem.* **1982**, *133*, 211.

(22) (a) Van De Mark, M. R.; Miller, L. L. *J. Am. Chem. Soc.* **1978**, *100*, 3223. (b) Oyama, N.; Anson, F. C. *J. Am. Chem. Soc.* **1979**, *101*, 739. (c) Oyama, N.; Anson, F. C. *J. Electrochem. Soc.* **1980**, *127*, 247.

(23) (a) Kaufman, F. B.; Schroeder, A. H.; Engler, E. M.; Kramer, S. R.; Chambers, J. Q. *J. Am. Chem. Soc.* **1980**, *102*, 483. (b) Daum, P.; Lenhard, J. R.; Rolison, D.; Murray, R. W. *J. Am. Chem. Soc.* **1980**, *102*, 4649. (c) Pickup, P. G.; Murray, R. W. *J. Am. Chem. Soc.* **1983**, *105*, 4510.

(24) Tamao, K.; Kodama, S.; Nakajima, I.; Kumada, M.; Minato, A.; Suzuki, K. *Tetrahedron* **1982**, *38*, 3347.

(25) Shu, C. F.; Wrighton, M. S. In *Electrochemical Surface Science: Molecular Phenomena at Electrode Surfaces*; Soriaga, M. P., Ed.; ACS Symposium Series, No. 378; American Chemical Society: Washington, 1988.

(26) Buchwald, S. L.; Wannamaker, M. W.; Watson, B. T. *J. Am. Chem. Soc.* **1989**, *111*, 776.

(5) Wightman, R. M. *Science* **1988**, *240*, 415.

(6) Lofion, E. P.; Thackeray, J. W.; Wrighton, M. S. *J. Phys. Chem.* **1986**, *90*, 6080.

(7) Feldman, B. J.; Burgmayer, P.; Murray, R. W. *J. Am. Chem. Soc.* **1985**, *107*, 872.

(8) Chao, S.; Wrighton, M. S. *J. Am. Chem. Soc.* **1987**, *109*, 6627.

(9) Garcia, E.; Kwak, J.; Bard, A. J. *Inorg. Chem.* **1988**, *27*, 4377.

(10) (a) Miller, L. L.; Mayeda, E. A. *J. Am. Chem. Soc.* **1970**, *92*, 5218. (b) Tinker, L. A.; Bard, A. J. *J. Am. Chem. Soc.* **1979**, *101*, 2316.

(11) Heinze, J.; Hinkelmann, K.; Dietrich, M.; Mortensen, J. *Ber. Bunsenges. Phys. Chem.* **1985**, *89*, 1225.

(12) Heinze, J.; Mortensen, J.; Hinkelmann, K. *Synth. Met.* **1987**, *21*, 209.

(13) Ofer, D.; Wrighton, M. S. *J. Am. Chem. Soc.* **1988**, *110*, 4467.

(14) Crooks, R. M.; Chyan, O. M. R.; Wrighton, M. S. *Chem. Mater.* **1989**, *1*, 2.

(15) Chance, R. R.; Boudreaux, D. S.; Brédas, J. L.; Silbey, R. In *Handbook of Conducting Polymers*; Skotheim, T. A., Ed.; Marcel Dekker: New York, 1986; Chapter 24.

cell or (experiments with $[(n\text{-Bu})_4\text{N}]\text{AsF}_6$ electrolyte) condensed onto P_2O_5 and distilled from the P_2O_5 onto Woelm activity I basic alumina. SO_2 was stored over the alumina until needed, at which time it was vacuum transferred to an electrochemical cell.

Electrochemical Cells. For conductivity change measurements in liquid SO_2 , vacuum tight single compartment cells were used.²⁷ In experiments where $[(n\text{-Bu})_4\text{N}]\text{PF}_6$ electrolyte was used, glassware was oven dried, assembled hot, loaded with electrolyte, and evacuated to 10^{-2} Torr while being heated to $\sim 120^\circ\text{C}$. Cells were opened and samples introduced under a back pressure of Ar and then evacuated to 10^{-2} Torr. SO_2 was condensed and experiments were run at -40°C (CH_3CN slush bath). In experiments where $[(n\text{-Bu})_4\text{N}]\text{AsF}_6$ electrolyte was used, cells were oven dried, assembled and loaded with electrolyte inside an inert atmosphere drybox, and evacuated to a final pressure of 10^{-5} – 10^{-6} Torr at $\sim 100^\circ\text{C}$. Then the evacuated cell and reference, counter, and working electrodes were taken into the drybox and assembled, and the cell was again evacuated to 10^{-5} – 10^{-6} Torr. SO_2 was condensed and experiments were run at -70°C (dry ice/*i*-PrOH bath).

For in situ spectroelectrochemical experiments in liquid SO_2 , vacuum tight cells based on a previously reported design²⁸ were used, with the optically transparent electrode (OTE) extending into a Pyrex cuvette encased in a Pyrex dewar with flat Pyrex windows. The dewar's cup contained a dry ice/*i*-PrOH mixture. An identical blank cell, containing the same liquid SO_2 /electrolyte concentration as the working cell and an undervivatized OTE, was positioned in the path of the spectrometer reference beam during experiments.

Electrodes. Arrays of eight individually addressable Pt microelectrodes ($\sim 50\ \mu\text{m}$ long, $\sim 0.1\ \mu\text{m}$ high, $\sim 2\ \mu\text{m}$ wide, and separated from each other by $\sim 1.2\ \mu\text{m}$) were fabricated and mounted by previously reported procedures.^{1,3} Where noted, the microelectrodes used were $\sim 3.6\ \mu\text{m}$ wide and separated from each other by $\sim 0.2\ \mu\text{m}$ and were fabricated by a shadow deposition technique.²⁹ Microelectrode arrays were cleaned and characterized prior to use. They were cleaned by either placing a drop of freshly mixed 3:1 concentrated H_2SO_4 –30% H_2O_2 directly on the array for 10 s and then rinsing with distilled H_2O or by O_2 plasma etching at 10^{-1} Torr and 300 W for 3 min. They were pretreated and characterized by cycling the individual microelectrodes of the array in 0.5 M H_2SO_4 between +1.2 and $-0.25\ \text{V}$ vs SCE until well-defined waves were observed in the hydrogen adsorption region.³⁰

Optically transparent electrodes were prepared by contacting a wire to tin doped indium oxide (ITO) coated glass (Delta Technologies) with Ag epoxy, and the Ag epoxy was then encapsulated in insulating epoxy. OTEs were cleaned prior to derivatization by sonicating for 10 min in acetone followed by 10 min in MeOH and then by O_2 plasma etching at 10^{-1} Torr and 300 W for 3 min. Pt wire or gauze counter electrodes were used, and oxidized Ag wires were used as quasireference electrodes.

Derivatization of Electrodes. Microelectrodes were derivatized with thiophene and pyrrole-based polymers by anodic polymerization^{31–33} of the appropriate monomer from 0.1 M solution in $\text{CH}_3\text{CN}/0.1\ \text{M} [(n\text{-Bu})_4\text{N}]\text{PF}_6$. Growth of polymer could be limited to a thickness sufficient to connect microelectrodes by the following procedure. The microelectrodes that were not to be derivatized were poised at a fixed potential negative of the monomer oxidation potential. The microelectrodes that were to be derivatized were scanned positive to a potential at which monomer oxidation yielded an anodic current of 2–10 mA/cm^2 . The microelectrodes were held at these potentials until drain current began to flow between derivatized and nonderivatized microelectrodes, indicating that the growing polymer film was beginning to connect them. At this point the polymer derivatized microelectrodes were, in the case of thiophene-based polymers, stepped negative to a potential at which the polymer was reduced to its neutral state or, in the case of pyrrole-based polymers, stepped to a potential negative of the oxidation potential for the monomer but at which the polymer remained significantly oxidized. The devices were then electrochemically characterized in fresh $\text{CH}_3\text{CN}/0.1\ \text{M} [(n\text{-Bu})_4\text{N}]\text{PF}_6$ and taken out of potential control in either a neutral (polythiophenes) or an oxidized (polypyrroles) state.

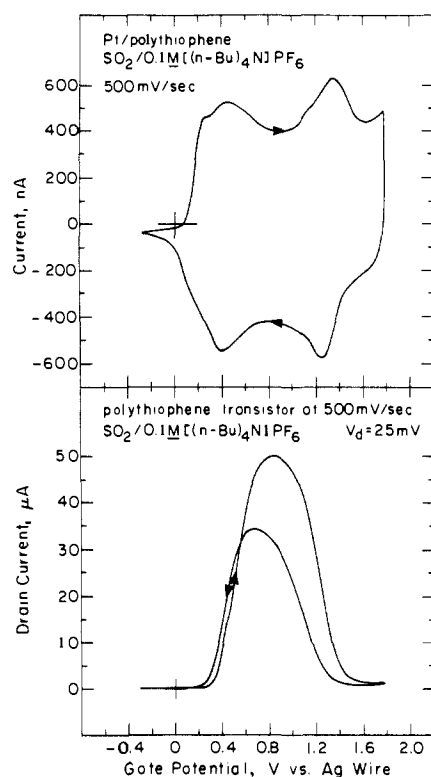


Figure 1. (Top) Cyclic voltammetry of I connecting three adjacent Pt microelectrodes in $\text{SO}_2/0.1\ \text{M} [(n\text{-Bu})_4\text{N}]\text{PF}_6$ at -40°C . Integration of the voltammogram indicates reversible removal of 7×10^{-7} mol of electrons per cm^2 of area covered by polymer. (Bottom) I_D – V_G characteristic in the same medium for an adjacent pair of microelectrodes connected with I for which cyclic voltammetry is shown. Maximum conductivity on the positive sweep is $\sim 10^{-1}\ \Omega^{-1}\ \text{cm}^{-1}$, and the window in which conductivity is at least 20% of maximum is 0.77 V wide.

Microelectrode arrays were derivatized with polyaniline by potential cycling as has been described previously^{1,34} and were characterized in 0.5 M NaHSO_4 . Polyaniline-derivatized microelectrodes were taken out of potential control at either $-0.2\ \text{V}$ vs SCE (polymer neutral and insulating) or $+0.5\ \text{V}$ vs SCE (polymer oxidized and conducting), rinsed repeatedly with HPLC grade H_2O , and then soaked in H_2O for 15 min and dried under vacuum. OTEs were derivatized by similar techniques.

Equipment. All electrochemical experiments were performed using a Pine Instruments RDE-4 bipotentiostat and data were recorded with a Kipp and Zonen BD91 x – y – y' recorder. Spectroscopic data were obtained using a Cary 17 UV–vis–near-IR spectrophotometer.

Results

a. Behavior of Thiophene-Based Polymers. Figure 1 shows cyclic voltammetry of a Pt microelectrode array derivatized with I. The electrolyte medium is liquid $\text{SO}_2/0.1\ \text{M} [(n\text{-Bu})_4\text{N}]\text{PF}_6$ at -40°C . The use of this medium allows chemically reversible oxidation to a much larger extent than in CH_3CN /electrolyte. In liquid SO_2 , the oxidized Ag wire quasireference electrode has a potential $\sim +0.4$ to $+0.5\ \text{V}$ vs SCE. The cyclic voltammogram shows an oxidation wave at $\sim 1.35\ \text{V}$ vs Ag which has not been previously observed. At the positive limit of the potential excursion the cyclic voltammogram shows increasing anodic current, but further oxidation leads to irreversible degradation of the polymer. Degradation is indicated by Coulombic irreversibility (additional charge passed is not recovered when the oxidized polymer is reduced) and by the irreversible loss of conductivity of the polymer.

Figure 1 also shows the I_D – V_G characteristic for the same microelectrode array operated in a transistor-like configuration. The important feature is that I_D , and therefore conductivity, significantly declines upon oxidation beyond $\sim 0.8\ \text{V}$ vs Ag, indicating that the polymer has a finite potential dependent window of high conductivity. This I_D – V_G characteristic is scan rate independent in the range 10^1 – $10^3\ \text{mV}/\text{s}$, and it is evident that large

(27) Bard, A. J.; Faulkner, L. R. *Electrochemical Methods*; Marcel Dekker: New York, 1980; p 25.

(28) Gaudiello, J. G.; Bradley, P. G.; Norton, K. A.; Woodruff, W. H.; Bard, A. J. *Inorg. Chem.* **1984**, *23*, 3.

(29) Jones, E. T. T.; Chyan, O. M.; Wrighton, M. S. *J. Am. Chem. Soc.* **1987**, *109*, 5526.

(30) Breiter, M.; Böld, W. *Electrochim. Acta* **1961**, *5*, 145.

(31) (a) Diaz, A. F.; Kanazawa, K. K.; Gardini, G. P. *J. Chem. Soc., Chem. Commun.* **1979**, 854. (b) Kanazawa, K. K.; Diaz, A. F.; Geiss, R. H.; Gill, W. D.; Kwak, J. F.; Logan, J. A.; Rabolt, J. F.; Street, G. B. *J. Chem. Soc., Chem. Commun.* **1979**, 653. (c) Wallman, R. J.; Bargon, J.; Diaz, A. F. *J. Phys. Chem.* **1983**, *87*, 1459.

(32) Tourillon, G.; Garnier, F. J. *Electroanal. Chem.* **1982**, *135*, 173.

(33) Tourillon, G.; Garnier, F. J. *Electroanal. Chem.* **1983**, *148*, 299.

(34) Diaz, A. F.; Logan, J. A. *J. Electroanal. Chem.* **1980**, *111*, 111.

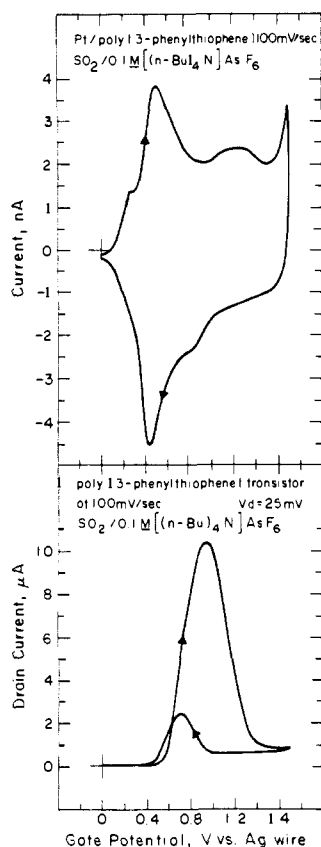


Figure 2. (Top) Cyclic voltammetry of III connecting two adjacent Pt microelectrodes in SO₂/0.1 M [(n-Bu)₄N]AsF₆ at -70 °C. Integration of the voltammogram indicates reversible removal of 1×10^{-7} mol of electrons per cm² of area covered by polymer. (Bottom) I_D - V_G characteristic in the same medium for the same pair of derivatized microelectrodes. Maximum conductivity on the positive sweep is $\sim 5 \times 10^{-2} \Omega^{-1} \text{cm}^{-1}$, and the window in which conductivity is at least 20% of maximum is 0.65 V wide.

changes in conductivity are correlated with peaks in the cyclic voltammogram. There is sweep rate independent hysteresis in the potential dependence of conductivity: the positive and the negative sweeps of the I_D - V_G trace do not show onset and decline of I_D at the same potentials, and this too correlates with hysteresis in the cyclic voltammetry. The maximum conductivity is lower on the negative sweep than on the positive sweep, and the magnitudes of I_D are reproducible on subsequent scans. The difference in conductivity for the positive and negative sweeps does not, therefore, result from degradation of the polymer. The cyclic voltammogram is also reproducible on subsequent scans, and this too indicates that the polymer does not undergo significant degradation under the conditions reported here.

Data for arrays derivatized with II or III (Figures 2 and 3) are very similar to those for the array derivatized with I. The use of the low-temperature SO₂/electrolyte medium allows reversible oxidation to potentials sufficiently positive to demonstrate an I_D - V_G characteristic that shows a finite potential window of high conductivity with conductivity changes coinciding with cyclic voltammetry peaks. Liquid SO₂ is not unique in this respect; a finite window of high conductivity can also be demonstrated for II in CH₂Cl₂/electrolyte (Figure 4). In CH₂Cl₂, the potential of the Ag wire quasireference electrode is ~ 0.5 V negative of its potential in liquid SO₂. However, highly oxidized II is less durable in CH₂Cl₂ than in liquid SO₂, with the positive potential sweep limit being dictated by the onset of rapid irreversible oxidation of the polymer and/or the medium at the potential of the more positive anodic cyclic voltammetry peak. It is noteworthy that in CH₂Cl₂ the separation between the more positive anodic and cathodic cyclic voltammetry peaks for II, and the associated hysteresis on the positive side of the I_D - V_G characteristic, is ~ 0.5 V, whereas in liquid SO₂ the hysteresis is ~ 0.2 V.

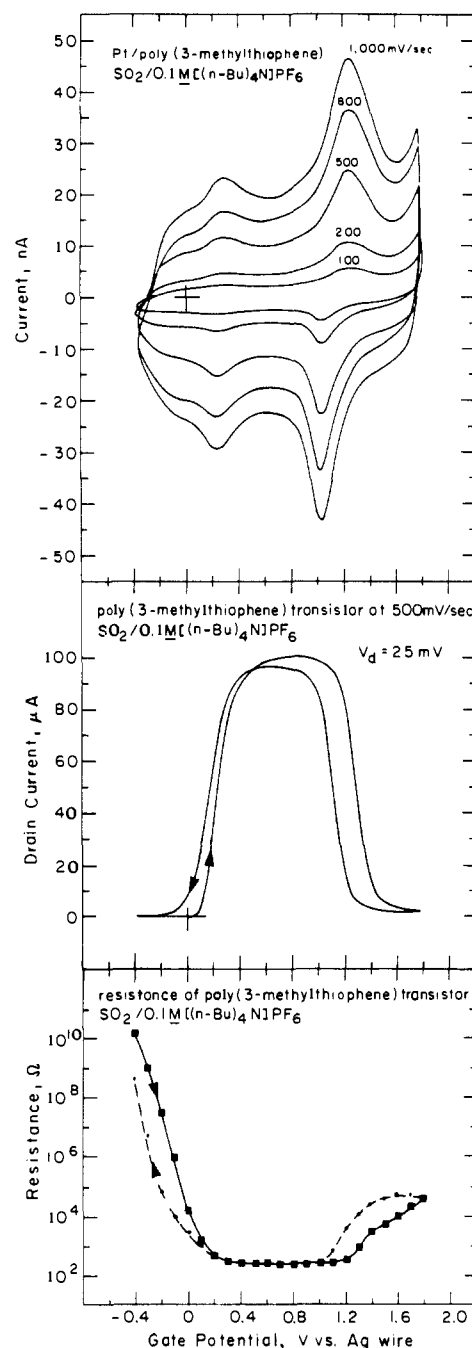


Figure 3. (Top) Cyclic voltammetry of II connecting three adjacent Pt microelectrodes in SO₂/0.1 M [(n-Bu)₄N]PF₆ at -40 °C. Integration of the voltammogram indicates reversible removal of 9×10^{-8} mol of electrons per cm² of area covered by polymer. (Middle) I_D - V_G characteristic in the same medium for an adjacent pair of microelectrodes for which cyclic voltammetry is shown. Maximum conductivity on the positive sweep is $\sim 10 \Omega^{-1} \text{cm}^{-1}$, and the window in which conductivity is at least 20% of maximum is 0.98 V wide. (Bottom) Steady-state resistance as a function of V_G for the same pair of microelectrodes for which the I_D - V_G characteristic is shown.

There are some differences in the behaviors of I, II, and III, but the essential features are the same: a finite region of high conductivity in the vicinity where substantial redox activity is found. Cyclic voltammograms for I-III in liquid SO₂ (Figures 1-3) all indicate that the amount of charge passed when the polymers are oxidized from the neutral insulating form to maximally conducting approximately equals that passed when they are further oxidized to the positive potential limit. But it is difficult to estimate the absolute extent of oxidation per thiophene repeat unit associated with conductivity changes in I-III, because it is difficult to determine how much polymer has been deposited on the microelectrode arrays in the anodic polymerization process.

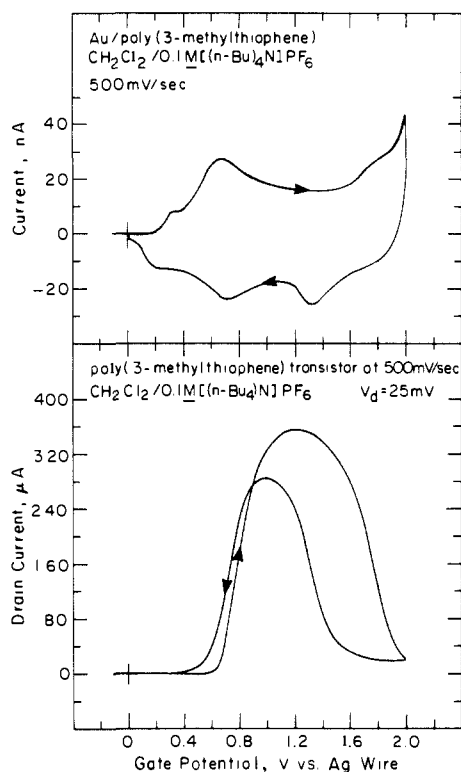


Figure 4. (Top) Cyclic voltammetry of II connecting six adjacent Au microelectrodes in $\text{CH}_2\text{Cl}_2/0.1 \text{ M } [(n\text{-Bu})_4\text{N}]\text{PF}_6$ at 25°C . Integration of the voltammogram indicates reversible removal of 8×10^{-8} mol of electrons per cm^2 of area covered by polymer. (Bottom) I_D - V_G characteristic in the same medium for an adjacent pair of microelectrodes for which cyclic voltammetry is shown.

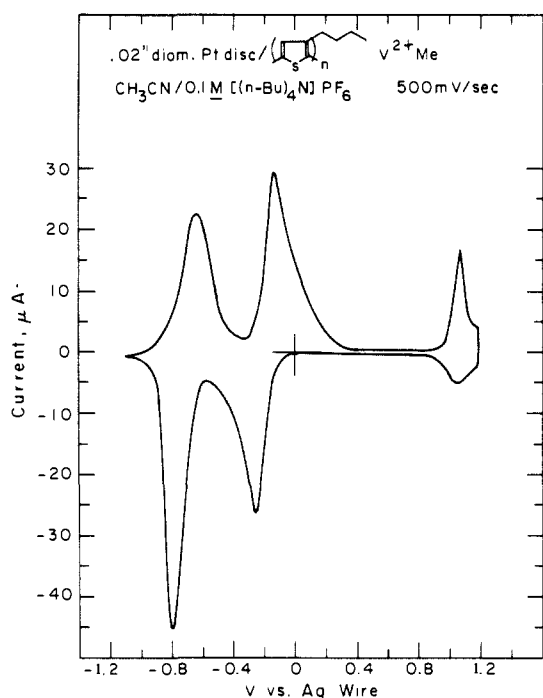


Figure 5. Cyclic voltammetry of IV on a 0.5 mm Pt disk electrode in $\text{CH}_3\text{CN}/0.1 \text{ M } [(n\text{-Bu})_4\text{N}]\text{PF}_6$ at 25°C .

Therefore a polymer made by electrochemical oxidation of 1-methyl-1'-(3-(thiophene-3-yl)propyl)-4,4'-bipyridinium (IV)²⁵ has been investigated. The total amount of polymer can be determined by integrating the cyclic voltammogram for the reversible reduction of its pendant *N,N'*-dialkyl-4,4'-bipyridinium (viologen) redox groups, because each viologen accepts an integral number of electrons upon reduction. Thus, the integration of the two,

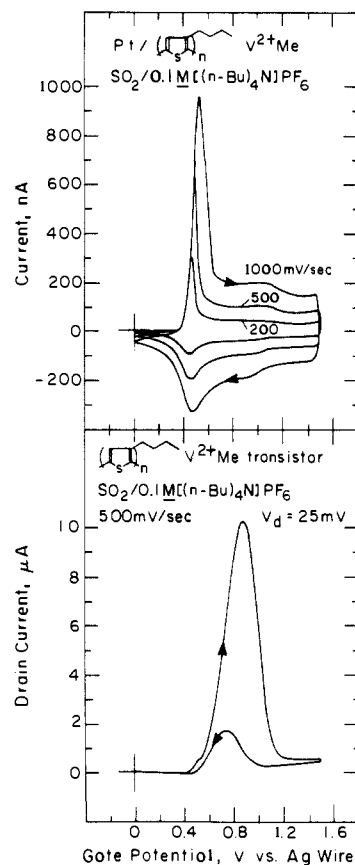


Figure 6. (Top) Cyclic voltammetry of IV connecting six adjacent Pt microelectrodes in $\text{SO}_2/0.1 \text{ M } [(n\text{-Bu})_4\text{N}]\text{PF}_6$ at -40°C . Assuming oxidation by ~ 0.25 electron per thiophene ring at $+0.6 \text{ V}$, integration of the voltammogram indicates 3×10^{-7} mol repeat unit per cm^2 of area covered by polymer. (Bottom) I_D - V_G characteristic in the same medium for the six microelectrodes in an interdigitated configuration (drain electrodes 2, 4, and 6 are offset $25 \text{ mV} = V_D$ from source electrodes 1, 3, and 5). Maximum conductivity on the positive sweep is $\sim 5 \times 10^{-3} \Omega^{-1} \text{ cm}^{-1}$, and the window in which conductivity is at least 20% of maximum is 0.47 V wide.

one-electron reduction waves yields the number of thiophene repeat units on the surface. The area of the voltammogram corresponding to oxidation of the polythiophene backbone can then be used to determine the extent of oxidation per thiophene repeat unit. Figure 5 shows the cyclic voltammogram of a Pt electrode derivatized with IV in $\text{CH}_3\text{CN}/0.1 \text{ M } [(n\text{-Bu})_4\text{N}]\text{PF}_6$. Integration of the viologen wave indicates coverage of 6×10^{-8} mol of repeat unit per cm^2 . At the positive potential limit used, the polythiophene backbone is oxidized to the extent of ~ 0.25 electron per thiophene ring. Figure 6 shows cyclic voltammetry and the I_D - V_G characteristic in liquid SO_2 of a microelectrode array derivatized with IV. Comparing the voltammogram of IV in SO_2 with that in CH_3CN , we estimate that IV in liquid SO_2 is oxidized by ~ 0.25 electron per thiophene ring at $+0.7 \text{ V}$ vs Ag. By integrating the voltammogram we estimate that at the anodic limit, $+1.5 \text{ V}$, IV is oxidized by ~ 0.5 electron per ring and that at the potential of maximum conductivity on the anodic sweep, $+0.86 \text{ V}$, IV is oxidized by ~ 0.3 electron per ring. Our results for IV are thus reasonably consistent with published data for the degree of oxidation for highly conducting samples of I and II which have been measured in the 0.15–0.5 electron per ring range by techniques including electrochemical methods,^{35–37} X-ray photoelectron spectroscopy,³⁸ and elemental microanalysis.^{32,39}

(35) Chung, T.-C.; Kaufman, J. H.; Heeger, A. J.; Wudl, F. *Phys. Rev. B* **1984**, *30*, 702.

(36) Colaneri, N.; Nowak, M.; Spiegel, D.; Hotta, S.; Heeger, A. J. *Phys. Rev. B* **1987**, *36*, 7964.

(37) Nagatomo, T.; Omoito, O. *J. Electrochem. Soc.* **1988**, *135*, 2124.

(38) Jugnet, Y.; Tourillon, G.; Duc, T. M. *Phys. Rev. Lett.* **1986**, *56*, 1862.

All of the thiophene-based polymers discussed so far, I–IV, have the same qualitative behavior: the neutral form is insulating, oxidation by ~ 0.3 electron per repeat unit yields the maximum conductivity, and further oxidation yields lower conductivity. However, some important differences exist among the four systems. The more positive cyclic voltammetry peaks for III and IV (Figures 2 and 6) are smaller than those for I and II (Figures 1 and 3). The conductivity changes associated with those peaks are also smaller for III and IV: significant I_D is evident at the positive V_G limit for III and IV, whereas for I and II, I_D returns to the base line at the positive limit. However, Figure 6 includes a plot of steady-state resistance for II as a function of V_G for the same derivatized microelectrodes for which the I_D – V_G data are shown. The method for measuring these resistances has been described previously.^{1,3,4} The data show that as II is oxidized to 0.8 V, the resistance between adjacent microelectrodes decreases by a factor of almost 10^8 , whereas when it is further oxidized to 1.8 V, resistance only increases by 10^2 – 10^3 . Similar results were obtained for I. The point is that for I and II, as well as for III and IV, the highly oxidized polymers cannot be made as resistive as the neutral polymers. Resistances for transistors based on III and IV are also about 10^{10} – 10^{11} Ω when V_G is at the negative limit. For these polymers, resistances at the positive V_G limit are obviously relatively low, as indicated by relatively large drain currents shown in the I_D – V_G characteristics.

One additional point regarding the data in Figure 3 needs to be addressed. The resistance measured includes the resistance of the microelectrode leads. When the polymer resistance is significantly greater than the lead resistance, the latter is unimportant. However, when lead resistance is significant compared to that of the polymer, the I_D – V_G data can be misleading. The minimum resistance of II is sufficiently small that the lead resistance does not introduce a problem. The leads typically have a 200–250 Ω resistance per pair of Pt microelectrodes. Therefore in Figure 3 this is essentially the resistance measured when II is most conductive. The point is that I_D is limited by the resistance of the leads for the peak currents shown in the I_D – V_G characteristic. On the basis of measurements of the microelectrode lead resistances and on other measurements with II-based transistors, we estimate that minimum polymer resistances for the device shown in Figure 3 are ~ 20 Ω , corresponding to a maximum conductivity of ~ 10 Ω^{-1} cm^{-1} . Therefore the conductivity of II actually changes by at least 10^9 on the negative side of the I_D – V_G peak and by almost 10^4 on the positive side. If I_D were limited by the resistance of the polymer alone and not by that of the leads, the peak I_D current would be about 10 times larger than actually observed in the I_D – V_G plot. In the case of I, we estimate that for the device shown in Figure 1, the actual minimum polymer resistance is 250–500 Ω , which would lead to a peak I_D about twice as large as that actually observed in the I_D – V_G plot. In the cases of III and IV, the microelectrode lead resistance is much smaller than the polymer resistance and does not significantly limit drain currents. The important observation regarding differences among the polythiophene systems is that the maximum conductivities and the widths of the potential windows of high conductivity both appear to follow the trend $\text{II} > \text{I} > \text{III} > \text{IV}$.

Polythiophenes I–IV, at the maximum positive potential in liquid SO_2 (limited by the onset of polymer degradation), are oxidized to an extent that is significantly less than 1 electron per thiophene repeat unit, *vide supra*. Large anodic currents at the positive potential limit indicate that the highest occupied band in each polymer still has significant electron population at this potential. Therefore, the polymers may be viewed as remaining in a "mixed valence" state yielding conductivity at the positive limit several orders of magnitude higher than for neutral polymers.

Optical absorption spectroscopy supports the conclusion that the polythiophenes are "mixed valence" at the most positive potential limits accessible. Figure 7 shows visible–near-infrared absorption spectra for II in liquid SO_2 /electrolyte at several potentials. The spectra were taken in order of increasingly positive

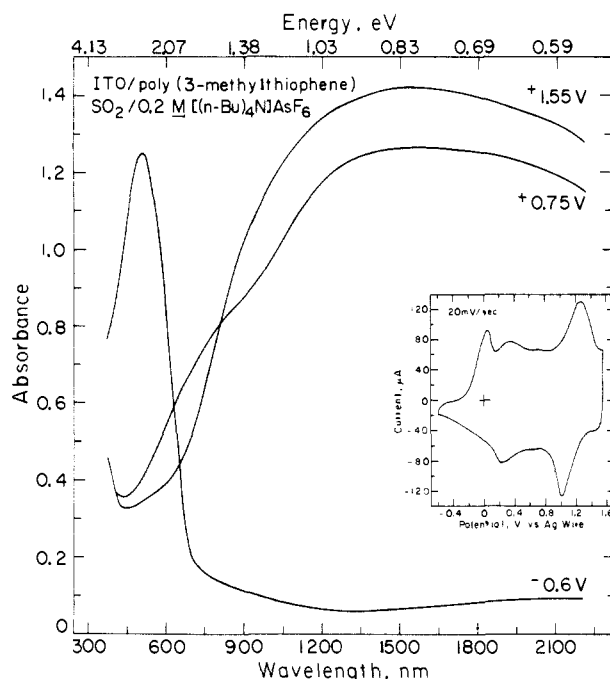


Figure 7. Visible–near-IR spectroelectrochemistry for II on ITO in $\text{SO}_2/0.2$ M $[(n\text{-Bu})_4\text{N}]\text{AsF}_6$ at -70 $^\circ\text{C}$. Inset: cyclic voltammetry of the same electrode in the spectroelectrochemical cell. Integration of the voltammogram indicates reversible removal of 2×10^{-7} mol of electrons per cm^2 of area covered by polymer.

potential, as in a positive sweep. The spectrum at -0.6 V is that known for neutral II, while the broad spectrum at $+0.75$ V (the potential of maximum conductivity) extends into the infrared and is similar to other spectra reported for highly conducting (oxidized) II.^{33,37,39,40} At $+1.55$ V, where the polymer is less conducting, the spectrum is quite similar to that at $+0.75$ V, indicating only a small change in electronic structure compared to the change in going from the neutral to the maximally conducting oxidized state. This is consistent with the highest occupied electronic band remaining partially populated at the most positive potential.

b. Behavior of Polyaniline in Liquid SO_2 . The behavior of polyaniline in liquid SO_2 /electrolyte (Figure 8) differs from that found for the polythiophenes. The cyclic voltammetry shows negligible faradaic current at the positive limit of potential excursion, indicating complete depopulation of the highest occupied electronic band. This, as shown by the plot of steady-state resistance vs V_G , is accompanied by a decline in conductivity to values similar to those for neutral polyaniline.

This contrast between the thiophene-based polymers and polyaniline is further defined by the differences in the spectroelectrochemistry for II (Figure 7) and for polyaniline (Figure 9). Figure 9 shows visible–near-infrared absorption spectra of polyaniline in liquid SO_2 /electrolyte at several potentials: -0.65 V where polyaniline is neutral (reduced) and insulating; $+0.35$ V where oxidized polyaniline has maximum conductivity; and $+1.35$ V where the oxidized polyaniline is very insulating. The spectra shown are similar to those that have previously been reported for polyaniline in varying degrees of oxidation and protonation.⁴¹ The

(39) Tourillon, G.; Garnier, F. *J. Phys. Chem.* **1983**, *87*, 2289.

(40) (a) Sato, M.; Tanaka, S.; Keeriyama, K. *Synth. Met.* **1986**, *14*, 279. (b) Hoier, S. N.; Ginley, D. S.; Park, S.-M. *J. Electrochem. Soc.* **1988**, *135*, 91. (c) Kaneto, K.; Hayashi, S.; Yoshino, K. *J. Phys. Soc. Jpn.* **1988**, *57*, 1119. (d) Patil, A. O.; Heeger, A. J.; Wudl, F. *Chem. Rev.* **1988**, *88*, 183. (41) (a) Kobayashi, T.; Yoneyama, H.; Tamura, H. *J. Electroanal. Chem.* **1984**, *161*, 419. (b) Stafström, S.; Brédas, J. L.; Epstein, A. J.; Woo, H. S.; Tanner, D. B.; Huang, W. S.; MacDiarmid, A. G. *Phys. Rev. Lett.* **1987**, *59*, 1464. (c) Epstein, A. J.; Ginder, J. M.; Zuo, F.; Bigelow, R. W.; Woo, H. S.; Tanner, D. B.; Richter, A. F.; Huang, W. S.; MacDiarmid, A. G. *Synth. Met.* **1987**, *18*, 303. (d) Shacklette, L. W.; Wolf, J. F.; Gould, S.; Baughman, R. H. *J. Chem. Phys.* **1988**, *88*, 3955. (e) Kim, Y. H.; Foster, C.; Chiang, J.; Heeger, A. J. *Synth. Met.* **1988**, *26*, 45. (f) Ohnawa, T.; Kabata, T.; Kimura, O.; Yoshino, K. *Synth. Met.* **1989**, *29*, E203.

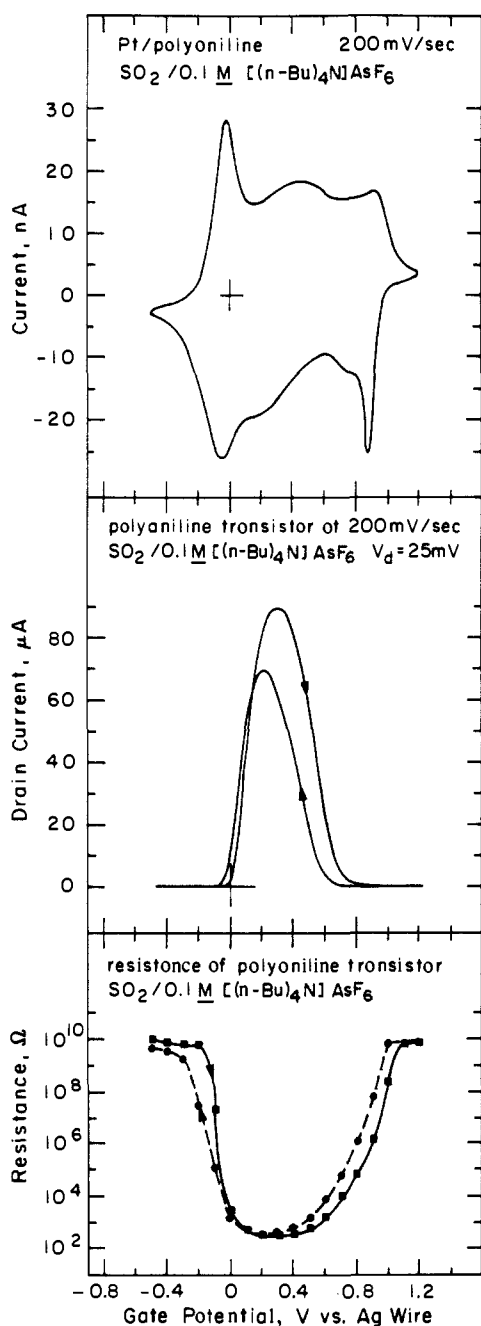


Figure 8. (Top) Cyclic voltammety of polyaniline connecting two adjacent Pt microelectrodes in $\text{SO}_2/0.1 \text{ M } [(n\text{-Bu})_4\text{N}]\text{AsF}_6$ over activity I basic alumina at -70°C . Integration of the voltammogram indicates 1.2×10^{-7} mol of repeat units per cm^2 of area covered by polymer. (Middle) I_D - V_G characteristic in the same medium for the same pair of derivatized microelectrodes. Maximum conductivity on the positive sweep is $\sim 1 \Omega^{-1} \text{cm}^{-1}$, and the window in which conductivity is at least 20% of maximum is 0.6 V wide. (Bottom) Steady-state resistance as a function of V_G for the same pair of derivatized microelectrodes.

neutral, insulating polymer absorbs only at high energy while the highly conductive film has intense, low-energy absorption trailing into the infrared, as found for II (Figure 7). However, in contrast to results for II, polyaniline shows negligible absorption in the near-infrared upon oxidation to the positive potential limit. The bleaching of the near-infrared absorption associated with high conductivity, together with the absence of faradaic current at the positive limit of the cyclic voltammogram, is consistent with essentially complete depopulation of the highest occupied electronic band of polyaniline at the positive potential limit.

The fact that oxidation of polyaniline to +1.35 V vs Ag yields complete removal of electrons from the highest occupied electronic band is consistent with findings showing reversible removal of one electron per repeat unit from polyaniline.¹⁶ The remarkable

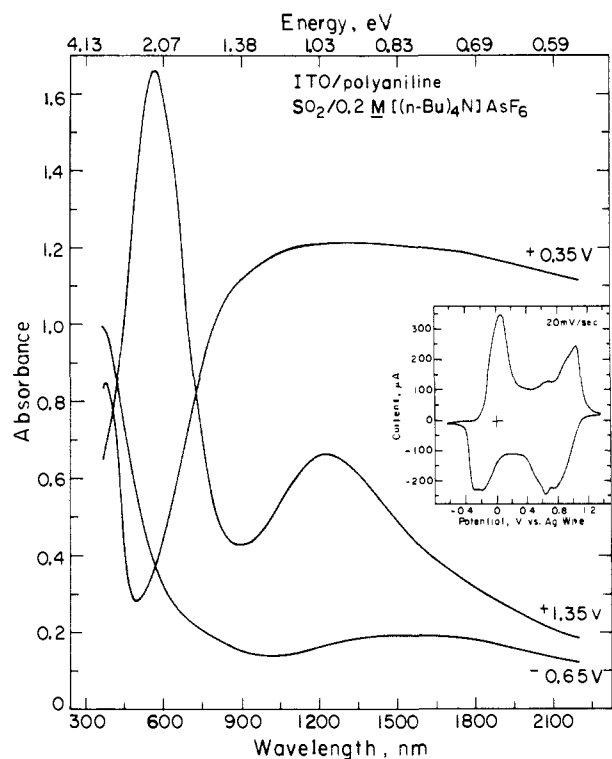


Figure 9. Visible-near-IR spectroelectrochemistry for polyaniline on ITO in $\text{SO}_2/0.2 \text{ M } [(n\text{-Bu})_4\text{N}]\text{AsF}_6$ at -70°C . Inset: cyclic voltammety of the same electrode in the spectroelectrochemical cell. Integration of the voltammogram indicates 3.4×10^{-7} mol of repeat units per cm^2 of area covered by polymer.

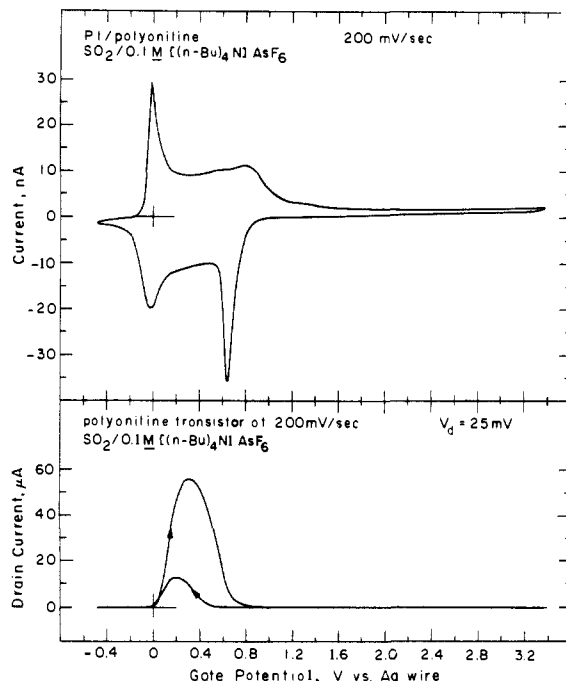


Figure 10. (Top) Cyclic voltammety of polyaniline connecting two adjacent Pt microelectrodes in $\text{SO}_2/0.1 \text{ M } [(n\text{-Bu})_4\text{N}]\text{AsF}_6$ over activity I basic alumina at -70°C . Integration of the voltammogram indicates 9.3×10^{-8} mol of repeat units per cm^2 of area covered by polymer. (Middle) I_D - V_G characteristic in the same medium for the same pair of derivatized microelectrodes.

durability of polyaniline in liquid SO_2 /electrolyte allows us to address the question of whether a deeper band is electrochemically accessible by going to a more positive potential. Figure 10 shows the cyclic voltammogram and corresponding I_D - V_G characteristic for polyaniline to a positive limit of 3.4 V vs Ag. Unfortunately, the liquid SO_2 /electrolyte medium precludes a more positive

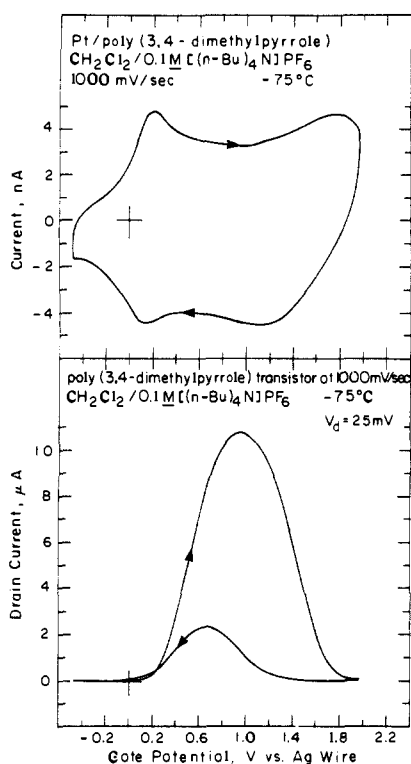


Figure 11. (Top) Cyclic voltammetry of V connecting two adjacent Pt microelectrodes in $\text{CH}_2\text{Cl}_2/0.1 \text{ M } [(n\text{-Bu})_4\text{N}]\text{PF}_6$ at -75°C . Integration of the voltammogram indicates reversible removal of 2×10^{-8} mol of electrons per cm^2 of area covered by polymer. (Bottom) I_D-V_G characteristic in the same medium for the same pair of derivatized microelectrodes. Maximum conductivity on the positive sweep is $\sim 5 \times 10^{-1} \Omega^{-1} \text{cm}^{-1}$, and the window in which conductivity is at least 20% of maximum is 1.2 V wide.

excursion, and we are unable to observe further oxidation of the polyaniline. Maintaining polyaniline in its fully oxidized state for prolonged periods does have some effect (but not an irreversible effect) on the polymer as shown by the negative scans of the Figure 10 plots. The negative scan of the cyclic voltammogram in Figure 10 shows the more positive cathodic peak at a potential negative of that observed when polyaniline is subjected to a less positive potential (Figure 8). Figure 10 also shows that there is a decline in conductivity as reflected by the relatively lower I_D in the negative scan of the I_D-V_G characteristic compared with that in Figure 8. However, these effects are reversed upon holding polyaniline at the potential of maximum conductivity. Thus, even though polyaniline does not undergo further electrochemical oxidation beyond $\sim 1.0 \text{ V}$ vs Ag, the material is remarkably durable to $+3.4 \text{ V}$ vs Ag.

There are differences in the cyclic voltammograms for polyaniline in liquid SO_2 shown in Figures 8–10 that merit some discussion. The cyclic voltammetry shown in Figure 9 resembles the voltammetry typically observed in aqueous acid media.^{1,42} The data in Figures 8 and 10 were collected under what were probably the most rigorously anhydrous and aprotic conditions used in our experiments, there having been activated basic alumina present in the bottom of the electrochemical cell, and the electrolyte having been dried in the cell at 100°C and 10^{-6} Torr. Under less dry conditions (no alumina in the cell, electrolyte less thoroughly dried, cell not evacuated to as low a final pressure before filling with SO_2), the cyclic voltammetry bears more resemblance to that in aqueous acid. This might be expected, given that water/ SO_2 solutions are known to be acidic.⁴³ However, the potential dependence of conductivity is essentially the same regardless of how

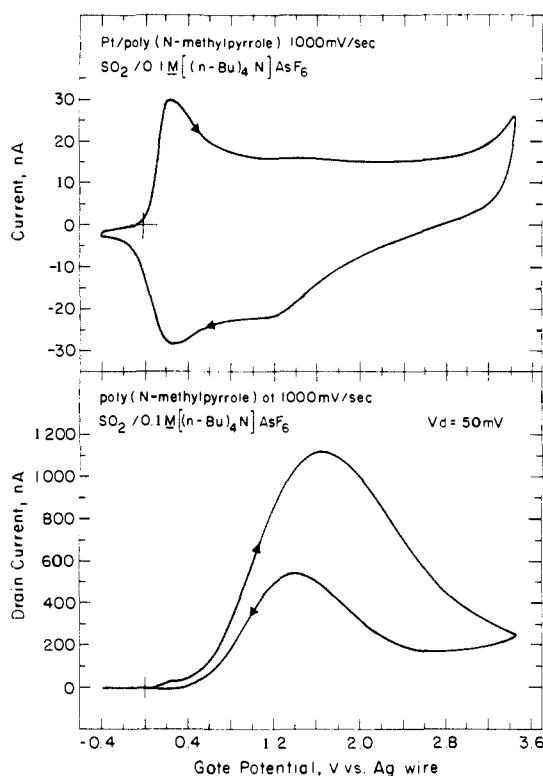


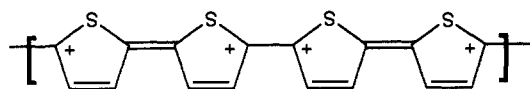
Figure 12. (Top) Cyclic voltammetry, in $\text{SO}_2/0.1 \text{ M } [(n\text{-Bu})_4\text{N}]\text{AsF}_6$ at -70°C , of V1 connecting two adjacent Pt microelectrodes having an interelectrode gap of 200 nm. Integration of the voltammogram indicates reversible removal of 1×10^{-7} mol of electrons per cm^2 of area covered by polymer. (Bottom) I_D-V_G characteristic in the same medium for the same pair of derivatized microelectrodes. Maximum conductivity on the positive sweep is $\sim 10^{-3} \Omega^{-1} \text{cm}^{-1}$. The window in which conductivity is at least 20% of maximum is at most 2.4 V wide (difficult to determine because of slow redox equilibration by polymer).

dry the SO_2 /electrolyte is. Indeed, the I_D-V_G plot for polyaniline is similar in $0.5 \text{ M H}_2\text{SO}_4$,¹ liquid SO_2 /electrolyte, and poly(vinyl alcohol)/ $\text{H}_3\text{PO}_4 \cdot n\text{H}_2\text{O}$.⁸ However, the positive potential limit in aqueous media is limited by rapid irreversible degradation beyond $\sim +0.8 \text{ V}$ vs SCE. Under the most anhydrous conditions in liquid SO_2 , holding polyaniline in its fully oxidized state has only a slight effect on its behavior (Figure 10). Under less anhydrous conditions, holding the polymer in its fully oxidized state causes conductivity to decline more rapidly and causes the most positive cyclic voltammetry peaks to shift further negative. The magnitude of both effects is roughly in proportion to the length of time for which the polymer is held fully oxidized. But remarkably, even when these effects are relatively severe, they are slowly reversed by cycling polyaniline through its full potential range of electroactivity or by just holding it at the potential of maximum conductivity. Last, the behavior of polyaniline is not influenced by the oxidation state it is in when transferred to the liquid SO_2 /electrolyte medium. Identical responses are observed for films that are taken out of potential control in aqueous acid solutions in either the neutral (insulating) or the 50% oxidized (conducting) states and then rinsed with pH 7 H_2O . Also, final rinsings with either $(\text{CH}_3\text{CH}_2)_3\text{N}$ or CH_3CN have no significant effect on the electrochemical response of polyaniline in liquid SO_2 /electrolyte.

c. Behavior of Pyrrole-Based Polymers. Figures 11 and 12 present data for poly(3,4-dimethylpyrrole) (V) and poly(N-methylpyrrole) (VI), showing that the potential dependence of their conductivity is much like that of the thiophene-based polymers. For V or for polypyrrole itself, which are relatively easily oxidized, the liquid SO_2 /electrolyte medium is not useful due to the relatively easy reduction of SO_2 . Figure 11 shows characterization of V in CH_2Cl_2 /electrolyte. The cyclic voltammogram of V has relatively large anodic and cathodic peaks at ~ 1.8 and $\sim 1.2 \text{ V}$, respectively. The anodic peak coincides with a decline in conductivity as the highly conducting polymer is

(42) Huang, W.-S.; Humphrey, B. D.; MacDiarmid, A. G. *J. Chem. Soc., Faraday Trans. 1* **1986**, *82*, 2385.

(43) Cotton, F. A.; Wilkinson, G. *Advanced Inorganic Chemistry*; John Wiley and Sons: New York, 1980; p 532.

Scheme II. Hypothetical Valence Structure for I Oxidized to the Extent of 1 Electron per Repeat Unit

further oxidized, and the cathodic peak coincides with a rise in conductivity as the highly oxidized polymer is reduced. The steady-state resistance of the polymer could not be measured in this potential regime because the durability of highly oxidized V is quite limited in CH_2Cl_2 , and therefore the data shown were collected at a fast scan rate with the solution cooled to near its freezing point. In order that the polymer remain in reasonable potential equilibrium with the electrode under these conditions, a particularly thin film of polymer was used. Though not shown, polypyrrole has an electrochemical response quite similar to that for V in the same medium.

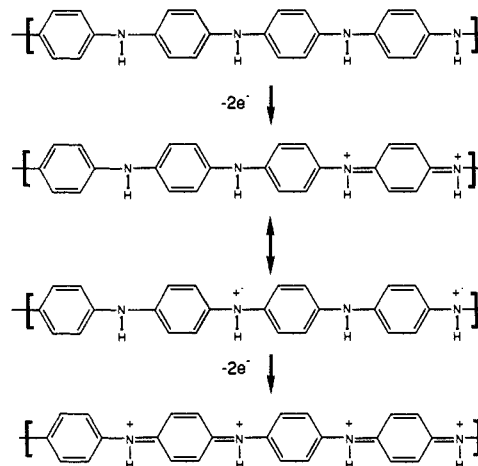
Figure 12 shows the characterization of VI in liquid SO_2 /electrolyte. The more positive anodic and cathodic cyclic voltammetry peaks, at ~ 1.6 and ~ 1.2 V, respectively, are not large, and neither are the associated changes in conductivity. The conductivity of highly oxidized VI at the positive potential limit is not less than 20% of its maximum conductivity on the positive sweep. In addition to having very limited durability when highly oxidized, VI also has a low maximum conductivity and slow redox kinetics in liquid SO_2 . Therefore microelectrode arrays with a smaller ($0.2 \mu\text{m}$) interelectrode gap²⁹ were used in order to lessen both the amount of polymer needed to connect electrodes and the length of the conduction path through the polymer. Even so, the cyclic voltammetry and I_D - V_G characteristic show a significant scan rate dependence. The width of the I_D - V_G characteristic at 200 mV/s is $\sim 12\%$ less than that at 1000 mV/s shown in Figure 12. Therefore the data in Figure 12 qualitatively demonstrate a finite potential window of high conductivity for oxidized VI but do not accurately show the width of the window. The pyrrole-based polymers are qualitatively similar to the thiophene-based polymers but are generally less durable and much less durable than polyaniline. The lack of ruggedness precludes detailed studies of pyrrole-based polymers at very positive potentials. Thus, studies of optical spectral changes have not been executed.

Discussion

A number of general observations can be made regarding the behavior of the polymers studied. First, it should be emphasized that the electrochemical responses recorded for the systems studied are reproducible. All can be demonstrated to have a finite potential window of high conductivity. Cyclic voltammetry shows that high conductivity occurs in the potential region where the polymer is redox active. This, together with optical spectroscopy, supports the conclusion that high conductivity is associated with partial depopulation of the highest occupied electronic band of the polymer and that it is therefore associated with a "mixed valence" state of fractional charge per repeat unit of the polymer.

The ability to define the potential window of high conductivity for a polymer hinges on its durability. The durability of the polymers discussed here varies under the experimental conditions used, but in general it is sufficient to allow reasonably accurate determination of the window of high conductivity. VI is the exception in that its electrochemical equilibration is too slow to allow it to be accurately characterized at the scan rates necessary to prevent degradation. It is noteworthy that only one of the polymers, polyaniline, is sufficiently rugged to allow its entire window of high conductivity to be studied.

The contrast between the durability of polyaniline when oxidized to the extent of 1 electron per repeat unit and the decomposition undergone by thiophene and pyrrole-based polymers when oxidized beyond ~ 0.5 electron per repeat unit may be explained by hypothetical valence structures for the "fully" oxidized polymers. Scheme II shows a polythiophene chain fully oxidized to the quinoid bipolaronic structures that, with varying degrees of delocalization, are believed to best represent the conformation

Scheme III. Hypothetical Structures of Polyaniline at Various Points in Its Redox Cycle in Liquid SO_2 ^a

^aTop: neutral and insulating. Middle: oxidized to 0.5 electron per repeat unit and highly conducting. Bottom: oxidized to 1 electron per repeat unit and insulating.

adopted by charged portions of a conjugated polyaromatic chain (similar structures apply to polypyrrole, polyparaphenylene, etc.).^{44,45} Although this picture may exaggerate the proximity into which adjacent charges might be forced, it is clear that oxidizing polythiophene to the extent of 1 electron per repeat unit should produce an extremely coulombically stressed and highly reactive structure. Polyaniline, however, has a larger repeat unit and nitrogen, with its relative affinity for positive charge, in conjugation. In fact it has been shown that in the protonated conducting form of polyaniline (Scheme III, middle), much of the charge resides on nitrogen atoms.⁴⁶ The known stability of the *p*-phenylenediamine dication⁴⁷ gives reason to expect that the structure shown at the bottom of Scheme III might be stable under appropriate conditions.

Scheme III is in fact a reasonable representation of the redox cycle of polyaniline in liquid SO_2 /electrolyte under sufficiently anhydrous conditions. Whereas mechanisms for the redox behavior in aqueous acid emphasize protonation and deprotonation,⁴² we judge that protonation/deprotonation does not play a role in liquid SO_2 . SO_2 is known to be less basic than ethylene in the gas phase,⁴⁸ and the anions of the electrolytes we have used are also extremely weak bases.⁴⁹ Therefore it is reasonable to assume that fully oxidized polyaniline (Scheme III, bottom) remains fully protonated.

The thiophene-based polymers appear to follow a trend in which the higher the conductivity of the polymer the wider its potential window of high conductivity. It is reasonable that these should be related, because the bandwidth of the highest occupied electronic band is a measure of delocalization in the system and should to some extent be correlated with both the charge carrier mobility¹⁸ and the width of the potential region over which the band can be depopulated. However, the band structure changes as the polymer is oxidized, and it may change in different ways for different polymers. This may be why such a trend is evident for thiophene-based polymers but not for pyrrole-based polymers. The fact that we find II to be the most highly conducting of the thiophene-based polymers I-IV is in accord with the prevailing literature. Possible reasons that have been mentioned previously⁵⁰ for the

(44) (a) Brédas, J. L.; Chance, R. R.; Silbey, R. *Mol. Cryst. Liq. Cryst.* **1981**, *77*, 319. (b) Brédas, J. L.; Thémans, B.; Fripiat, J. G.; André, J. M.; Chance, R. R. *Phys. Rev. B* **1984**, *29*, 6761.

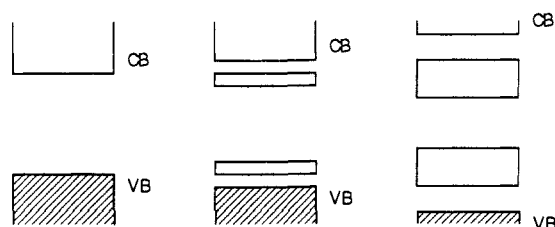
(45) Brédas, J. L.; Street, G. B. *Acc. Chem. Res.* **1985**, *18*, 309.

(46) Kaplan, S.; Conwell, E. M.; Richter, A. F.; MacDiarmid, A. G. *J. Am. Chem. Soc.* **1988**, *110*, 7647.

(47) Yao, T.; Musha, S.; Munemori, M. *Chem. Lett.* **1974**, 939.

(48) Collyer, S. M.; McMahon, T. B. *J. Phys. Chem.* **1983**, *87*, 909.

(49) Gordon, A. J.; Ford, R. A. *The Chemist's Companion*; John Wiley and Sons: New York, 1976; p 60.

Scheme IV. Hypothetical Evolution of Band Structure upon Oxidation of a Polyaromatic Conducting Polymer^a

^a Left: neutral polymer with filled valence band, VB, and empty conduction band, CB. Middle: band structure at relatively low extent of oxidation. Valence band remains full and holes are accommodated in new bands that grow in the gap. Right: band structure at higher extent of oxidation. More states are added to bands in the gap while valence and conduction bands shrink.

differing conductivities of various thiophene-based polymers include steric effects, electronic factors, and differences in the polymerizations of the respective monomers. In our work we caution against conclusions regarding such influences because of the lack of detailed information concerning the structure of the polymers.

For all the polymers studied, the conductivity changes on the positive side of the I_D - V_G characteristic are accompanied by cyclic voltammetry peaks. That is, an anodic peak in the voltammogram is associated with decline in conductivity when the oxidized, highly conducting, polymer is further oxidized, and a cathodic peak in the voltammogram is associated with increase in conductivity when the less conducting, highly oxidized, polymer is reduced. In general, it appears that the larger the changes in conductivity are, the larger the voltammetric peaks. This might be expected because changes in the conductivity of the polymer are associated with changes in the extent of delocalization of the highest energy electrons in the polymer. The more highly conducting the polymer is, the more delocalized the highest energy electrons should be and the greater the extent to which removal of any one electron lowers the energies of the others. In this state, the polymer should behave as a metal in the sense of its having a broad potential region of continuous charging. However, as conductivity declines and the highest energy electrons become more localized, the redox behavior of the polymer should approach that of an ensemble of noninteracting redox units as in conventional redox polymers like polyvinylferrocene.⁵¹ Under such circumstances, removal of any one of the highest energy electrons should have little effect on energies of the others, and the voltammogram should have a peak, as a large number of non-interacting electrons with the same energy are removed at once.

All the polymers have cyclic voltammograms and I_D - V_G plots showing significant hysteresis. The hysteresis is typically greater on the positive side of the potential of maximum conductivity than on the negative side. Hysteresis in all the potential dependent properties of conducting polymers has been explained as a result of changes in polymer structure that causes excess charge to reside in new electronic levels located in the band gap.^{35,52} Therefore charge is injected at potentials corresponding to the band edges (top of the valence band for oxidation of neutral polymers, bottom of the conduction band for reduction of neutral polymers) but is neutralized at potentials corresponding to the new levels located in the gap. Hysteresis in the potential-dependent properties of an oxidized conducting polymer can then be a measure of the energy gap between the top of the valence band and the bottom of the lowest band in the gap when the polymer is oxidized to some

given extent. Our data suggest that, as illustrated in Scheme IV, this energy gap, and therefore hysteresis, increases as the polymer is oxidized to a greater extent. Such an evolution of the band structure upon oxidation has been calculated for polypyrrole.⁴⁵ A widening of the energy gap between the upper edge of the occupied valence band and the lower edge of the bands in the gap may be due to narrowing of the bands associated with the increased localization of charge as the highly oxidized polymer becomes less conducting. Spectroscopic absorption edges in the infrared corresponding to this energy gap have been reported for a number of oxidized conducting thiophene-based polymers^{39,53} and for polyaniline.⁵⁴ Studies of infrared spectroelectrochemistry and EPR measurements of conducting polymers in liquid SO_2 /electrolyte are in progress. These studies will help to further define the behavior of the conducting polymers and to provide insight regarding the best theoretical description^{15,19,35,36,44,55,56} of these systems in their various states of charge.

The I_D - V_G characteristics of the polymers studied show higher maximum I_D , and therefore higher maximum conductivity, for the positive sweep than for the negative sweep. This may result from the overcoming of a kinetic barrier to charge localization within the polymer during the oxidation process. As the polymer becomes highly oxidized, Coulombic repulsions could drive the polymer chains to adopt conformations in which discrete segments stabilize more localized charges, and these segments are then less involved in conduction upon reduction of the oxidized polymer.

Recent work reporting that slight changes in solvent polarity can significantly influence the extent of spin pairing in oxidized, soluble poly(3-hexylthiophene)⁵⁶ suggests that intrachain Coulombic repulsions, and their screening by solvent and electrolyte reorganization, can play a large role in the dynamics of oxidation and charge distribution in conducting polymers. It might be expected that the effects of Coulombic repulsions between polymer charge sites and their screening by solvent/electrolyte will increase as the extent of oxidation of a conducting polymer is increased. Such effects might be particularly significant in the very positive potential region, where the decline of polymer conductivity and the increase of charge localization may in part be due to a higher density of charge in the polymer. This may be relevant to the differences between the potential-dependent characteristics of II in liquid SO_2 and in CH_2Cl_2 (Figures 3 and 4). On the negative side of the I_D - V_G characteristic, the potential-dependent behavior of II in CH_2Cl_2 is similar to that in SO_2 . This would be consistent with the expectation that the relative effects of different solvents in screening intrapolymer Coulombic repulsions would be less significant at lower charge densities. However, in the more positive potential region where the polymer has a higher density of charge, the hysteresis observed in the cyclic voltammograms and I_D - V_G characteristics is very different for the two solvent systems. These differences are likely a reflection of differences in the solvation of the reduced and oxidized polymer in the two solvent systems.

In summary, the observation of a finite potential window of high conductivity for oxidized polythiophenes and polypyrroles, as was previously found for polyaniline, suggests that this is a general feature of conducting organic conjugated polymers and that high conductivity in these systems is associated with "mixed valence" states of fractional charge per repeat unit. The use of appropriate solvent/electrolyte systems that extend the potential regime in which conducting polymers can be investigated reveals characteristic effects that should aid in developing a better understanding of their behavior. The use of microelectrode arrays

(53) Gustafsson, G.; Inganäs, O.; Nilsson, J. O.; Liedberg, B. *Synth. Met.* **1988**, *26*, 297.

(54) (a) Sariciftci, N. S.; Kuzmany, H.; Neugebauer, H.; Neckel, A. J. *Chem. Phys.* **1990**, *92*, 4530.

(55) (a) Chen, J.; Heeger, A. J.; Wudl, F. *Solid State Commun.* **1986**, *58*, 251. (b) Brédas, J. L.; Wudl, F.; Heeger, A. J. *Solid State Commun.* **1987**, *63*, 557. (c) Schärli, M.; Kiess, H.; Harbecke, G.; Berlinger, W.; Blazey, K. W.; Müller, K. A. *Synth. Met.* **1988**, *22*, 317. (d) Lögdlund, M.; Lazzaroni, R.; Stafström, S.; Salaneck, W. R.; Brédas, J.-L. *Phys. Rev. Lett.* **1989**, *63*, 1841.

(56) Nowak, M. J.; Spiegel, D.; Hotta, S.; Heeger, A. J.; Pincus, P. A. *Macromolecules* **1989**, *22*, 2917.

(50) (a) Bureau, J. M.; Gazard, M.; Champagne, M.; Dubois, J. C.; Tourillon, G.; Garnier, F. *Mol. Cryst. Liq. Cryst.* **1985**, *118*, 235. (b) Roncali, J.; Lemaire, M.; Garreau, R.; Garnier, F. *Synth. Met.* **1987**, *18*, 139. (c) Hotta, S. *Synth. Met.* **1987**, *22*, 103. (d) Roncali, J.; Garreau, R.; Yassar, A.; Marque, P.; Garnier, F.; Lemaire, M. *J. Phys. Chem.* **1987**, *91*, 6706.

(51) Flanagan, J. B.; Margel, S.; Bard, A. J.; Anson, F. C. *J. Am. Chem. Soc.* **1978**, *100*, 4248.

(52) Kaufman, J. H.; Kaufer, J. W.; Heeger, A. J.; Kaner, R.; MacDiarmid, A. G. *Phys. Rev. B* **1982**, *26*, 2327.

to measure potential-dependent changes in conductivity allows such measurements to be made rapidly in potential regimes where the polymers may have very limited durability.

Acknowledgment. We thank the Office of Naval Research, the Defense Advanced Research Projects Agency, and the National Science Foundation through the M.I.T. Materials Research

Laboratory for partial support of this research. We thank Professor Robert J. Silbey for several valuable discussions and we thank Dr. Timothy M. Miller for providing us with 3-phenylthiophene, Professor Stephen L. Buchwald for providing us with 3,4-dimethylpyrrole, and Dr. Ching-Fong Shu for providing us with 1-methyl-1'-(3-(thiophene-3-yl)propyl)-4,4'-bipyridinium-2PF₆⁻.

The Use of an Electrogenerated Cobalt(I) Porphyrin for the Homogeneous Catalytic Reduction of Dioxygen in Dimethylformamide. Reactions of [(TMpyP)Co^{II}]⁴⁺ and [(TMpyP)Co^I]³⁺ Where TMpyP = *meso*-Tetrakis(1-methylpyridinium-4-yl)porphyrin

D. Sazou, C. Araullo-McAdams, B. C. Han, M. M. Franzen, and K. M. Kadish*

Contribution from the Department of Chemistry, University of Houston, Houston, Texas 77204-5641. Received April 24, 1990

Abstract: The one-electron catalytic reduction of dioxygen by electrogenerated *meso*-tetrakis(1-methylpyridinium-4-yl)-porphyrinatocobalt(I), [(TMpyP)Co^I]³⁺, was investigated by cyclic voltammetry, controlled potential coulometry, rotating ring-disk voltammetry, ESR, and UV-visible spectroelectrochemistry. The first reduction of [(TMpyP)Co^{II}]⁴⁺ in DMF containing 0.1 M tetrabutylammonium perchlorate occurs at $E_{1/2} = -0.49$ V and leads to the formation of [(TMpyP)Co^I]³⁺. This cobalt(I) complex is stable under an N₂ atmosphere but in the presence of dissolved O₂ is converted to [(TMpyP)Co^{II}(O₂-)]³⁺, which is also stable at all potentials up to the reduction of free O₂ (i.e., about -0.80 to -0.90 V vs SCE). A catalytic reduction of dioxygen occurs at $E_p = -0.50$ V by cyclic voltammetry (scan rate = 0.1 V s⁻¹) in DMF solutions containing [(TMpyP)Co^{II}]⁴⁺ and benzoic anhydride under O₂. The homogeneous reactions of [(TMpyP)Co^{II}]⁴⁺ and electrogenerated [(TMpyP)Co^I]³⁺ with O₂ or O₂⁻ were characterized and monitored by ESR and UV-visible spectroscopic techniques. A high oxidation state cobalt complex was spectrally characterized during reduction of [(TMpyP)Co^{II}]⁴⁺ in DMF solutions containing O₂ and benzoic anhydride, while the addition of cyclohexene to this mixture led to the generation of cyclohexene oxide. Integration of the current time curves for reduction of [(TMpyP)Co^{II}]⁴⁺ in DMF containing benzoic anhydride under O₂ gave a turnover number of ~15 during the first 15 min of bulk electrolysis. The calculated number of turnovers for the conversion of cyclohexene to cyclohexene oxide was 55 during 4.5 h of electrolysis and suggests that the investigated cobalt porphyrin is an extremely efficient catalyst for the reduction of O₂ or the electrocatalytic epoxidation of alkenes.

Introduction

Numerous complexes of water soluble iron(II),¹⁻⁶ cobalt(II),⁷⁻¹² and manganese(II)¹³ porphyrins have been used as catalysts for the multielectron reduction of dioxygen. This reaction can proceed via two electrons to yield hydrogen peroxide or four electrons to

give water as the final product in aqueous solutions.

Examples for the electrocatalytic reduction of oxygen by metalloporphyrins are extensive, but very little work has been carried out in nonaqueous organic solvents where the one-electron reduction of free O₂ will generate superoxide anion.^{14,15} In fact, only a few examples for the catalytic reduction of O₂ by metalloporphyrins in nonaqueous media have been published.¹⁶⁻¹⁸ These studies utilized a Mn(II) porphyrin as the catalyst which, during the reaction, was converted to an intermediate high oxidation state Mn(V) species^{16,17} or to a mixed-valent dimeric manganese Mn(III)/Mn(IV) complex.¹⁸

The majority of studies involving catalytic reduction of O₂ by cobalt porphyrins have utilized cobalt(II) complexes as catalysts for the heterogeneous reduction of dioxygen to hydrogen peroxide^{19,20} or water²¹ in aqueous media. This present study also

(1) Ozer, D.; Harth, R.; Mor, U.; Bettelheim, A. *J. Electroanal. Chem.* **1989**, *266*, 109.

(2) Kuwana, T.; Fujihira, M.; Sunakawa, K.; Osa, T. *J. Electroanal. Chem.* **1978**, *88*, 299.

(3) Bettelheim, A.; Kuwana, T. *Anal. Chem.* **1979**, *51*, 2257.

(4) Forshey, P. A.; Kuwana, T. *Inorg. Chem.* **1981**, *20*, 693.

(5) Shigehara, K.; Anson, F. C. *J. Phys. Chem.* **1982**, *86*, 2776.

(6) Bettelheim, A.; Chan, R. J. H.; Kuwana, T. *J. Electroanal. Chem.* **1980**, *110*, 93.

(7) Bettelheim, A.; Chan, R. J. H.; Kuwana, T. *J. Electroanal. Chem.* **1979**, *99*, 391.

(8) Haase, J. Z. *Naturforsch., A* **1968**, *23*, 1000.

(9) Forshey, P. A.; Kuwana, T.; Kobayashi, N.; Osa, T. *Adv. Chem. Ser.* **1982**, *201*, 601.

(10) Durand, R. R., Jr. Ph. D. Thesis, California Institute of Technology, **1984**.

(11) Ozer, D.; Parash, R.; Broitman, F.; Mor, U.; Bettelheim, A. *J. Chem. Soc., Faraday Trans. 1* **1984**, *80*, 1139.

(12) Ni, C.-L.; Anson, F. C. *Inorg. Chem.* **1985**, *24*, 4754.

(13) Bettelheim, A.; Ozer, D.; Parash, R. *J. Chem. Soc., Faraday Trans. 1* **1983**, *79*, 1555.

(14) Maricle, D. L.; Hodgson, W. G. *Anal. Chem.* **1965**, *37*, 1562.

(15) Sawyer, D. T.; Roberts, J. L., Jr. *J. Electroanal. Chem.* **1966**, *12*, 90.

(16) Creager, S. E.; Raybuck, S. A.; Murray, R. W. *J. Am. Chem. Soc.* **1986**, *108*, 4225.

(17) Creager, S. E.; Murray, R. W. *Inorg. Chem.* **1987**, *26*, 2612.

(18) Perrée-Fauvet, M.; Gaudemer, A.; Bonvoisin, J.; Girerd, J. J.; Boucly-Goester, C.; Boucly, P. *Inorg. Chem.* **1989**, *28*, 3533.

(19) Durand, R. R.; Anson, F. C. *J. Electroanal. Chem.* **1982**, *134*, 273.

(20) Chan, R. J. H.; Su, Y. O.; Kuwana, T. *Inorg. Chem.* **1985**, *24*, 3777.